Earthquake Geotechnical Engineering, Ishihara (ed.) © 1995 Balkema, Rotterdam. ISBN 90 5410 578 X

Microtremor observation at Hualien LSST array site, Taiwan

M.A.Ansary & F.Yamazaki
Institute of Industrial Science, University of Tokyo, Japan

T.Kokusho & T.Ueshima
Central Research Institute of Electric Power Industry, Abiko, Japan

ABSTRACT: Hualien LSST array is situated in a stiff soil site in Hualien, Taiwan. This is the first study using microtremor measurement at the site to predict soil chracteristics and earthquake ground motion. Short-period microtremors were observed as arrays and points both in the free-field as well as in the backfill to compare their amplification characteristics. Apparent velocities were also estimated from the FK-spectrum analysis of microtremor arrays.

1 INTRODUCTION

Recently a large number of seismograph arrays[1-3] have been installed all around the world to study the effect of local topography and geology on amplification and spatial variation of earthquake ground motion. However, accumulation of strong ground motion data takes some time before comprehensive analysis can be done.

Microtremor observation[4-6] is a popular tool to evaluate dynamic response characteristics of structures and ground, especially in Japan. Microtremors contain a wide range of frequencies and can be measured at any time and for any duration. Discussions still remain about the source and type of waves constituting the microtremors.

This study analyses the spectral characteristics of microtremor measured at several points near the existing surface accelerometers of Hualien LSST array[3], situated at a stiff soil site in Taiwan. These results are compared with those of earthquake ground motion. The dispersion curve obtained by an FK-spectrum analysis of the microtremor array data is compared with the theoretical curve using the existing underground model.

2 HUALIEN LSST AND ITS STRONG MOTON DATA

Since 1992, a accelerometer array has been in operation in Hualien LSST site, which is situated along the east coast of Taiwan. The location of the array is shown in Figure 1. This is a joint research project of USA, Taiwan, Japan, France and Korea. In this array, a number of accelerometers are placed in 3 boreholes and on the surface, as shown in Figures 2 and 3.

The analysis was performed using the data currently available from three earthquakes, which occurred in 1994. Basic information about these events is presented in Table 1. These records are corrected recently for orientation errors[7] and for this study corrected earthquake records were used.

3 LOCAL GEOLOGY AND SITE CONDITION

The general geology in Hualien consists of massive unconsolidated, poorly bedded conglomerative composed of pebbles varying in diameter from 10 to 20 centimeter[3]. The subsurface ground till almost 5 m depth was mainly composed of fine and /or medium sand, and it includes fine sand 1.5 m thickness, medium sand with boulders of 1 m thickness and medium fine sand with 2 m thickness. Gravel layer was encountered at a depth of about 5 m below the ground surface, and its existence was confirmed down to a depth of 40 m. The ground water table is located at a depth of about 2 m in this site.

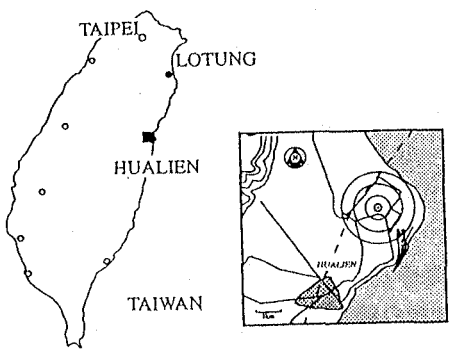

Fig. 1 Location of Hualien LSST site

Table 1. Information on the earthquake records

Event	Mag.	Lat.	Long.	Depth (km)	Max. acc. at A15 (cm/s²)
EQ940120	5.6	24°03'36"N	121°51'00"N	49.50	43.06
EQ940530	4.5	24°05'40"N	121°34'20"N	18.50	34.12
EQ940605	6.2	24°27'60"N	121°50'40"N	5.30	42.34

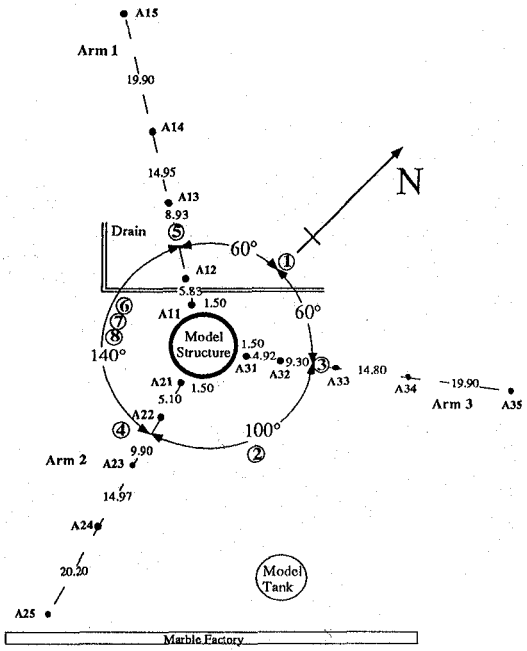

Orientation of Sensors
caseA: 6 NS; 7 EW; 1,2,3,4,5,8 UD
caseB: 1,2,3,4,5,6 NS; 7 EW; 8 UD
Note: All the dimensions are in meters

Fig. 2 Location of the surface seismometers and position of microtremor pickups for a particular array dimension

A number of geophysical measurement program have been conducted to determine shear wave and compressional wave velocities[8]. The investigations employed cross-hole, down-hole and suspension methods. Scoping geophysical and boring tests conducted in 1989 by Taipower show that the shear wave velocity for the top layer of 100 m depth is around 400 m/s and for the layer below (upto 7 km depth) is 1500 to 1850 m/s. Figure 4 shows the unified soil model[9] and the model structure. Tables 2, 3 and 4 describe the soil conditions at sections 1, 2 and 3 of the unified model, respectively.

4 MICROTREMOR OBSERVATION IN FREE-FIELD

The instrument used for the microtremor measurement was SPC-35T (Tokyo Sokushin Co.). The velocity records obtained by the sensors are highpass-filtered, amplified (amplifier: 8 channels) and converted to digital recording using a 16 bit AD converter for

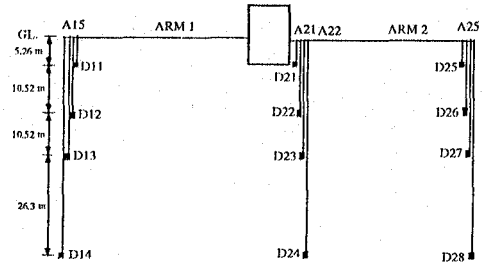

Fig. 3 Location of borehole seismometers

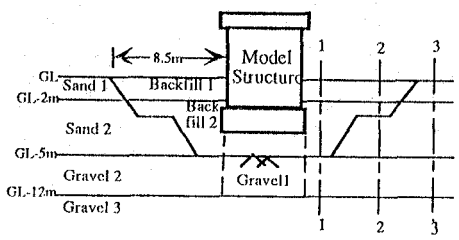

Fig. 4 Unified soil model (CRIEPI, 1993)

Table 2 The Unified Model at section 1 (near the model structure)

Layer No.	Layer (m)	Vs (m/s)	ρ (g/cm²)	ν	E (kgf/m²)	No. of sublayers
1	0 - 2	400	2.33	0.38	1.030	1
2	2 - 5	400	2.39	0.48	1.130	1
3	5 - 12	333	2.42	0.47	0.790	1
4	12 - 48	476	2.42	0.47	1.612	2
5	48 - 70	540	2.42	0.47	2.075	2
6	70 - 117	515	2.42	0.47	1.887	3
7	117 - 160	620	2.42	0.47	2.735	3
8	160 - 176	665	2.42	0.47	3.146	2
9	176 - 2000	890	2.42	0.47	5.636	4

Table 3 The Unified Model at section 2 (4.0-8.5 m away from the model structure)

Layer No.	Layer (m)	Vs (m/s)	ρ (g/cm²)	ν	E (kgf/m²)	No. of sublayers
1	0 - 2	400	2.33	0.38	1.030	1
2	2 - 2.5	400	2.39	0.48	1.130	1
3	2 - 5	231	1.93	0.48	0.305	1
Layers 4 to 10 are same as Layers 3 to 9 in Table 2						

Table 4 The Unified Model at section 3 (in the free-field)

Layer No.	Layer (m)	Vs (m/s)	ρ (g/cm²)	ν	E (kgf/m²)	No. of sublayers
1	0 - 2	133	1.69	0.38	0.083	1
2	2 - 5	231	1.93	0.48	0.305	1
Layers 3 to 9 are same as in Table 2						

storage in the hard disk of the personal computer. For velocity, sensitivity of the instrument is flat for period less than about 1 s. For this study, sampling frequency of 100 Hz was used.

Figure 2 shows the site plan along with the location of surface accelerometers (points with letter A are

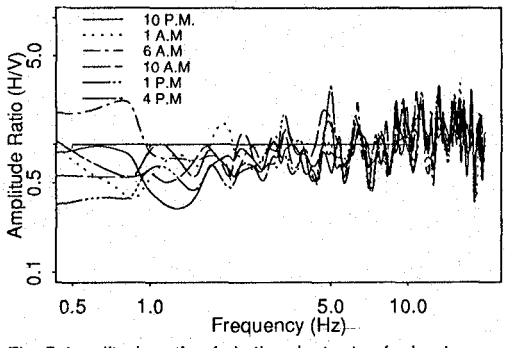

Fig. 5 Amplitude ratio of six time instants of microtremor at the reference point

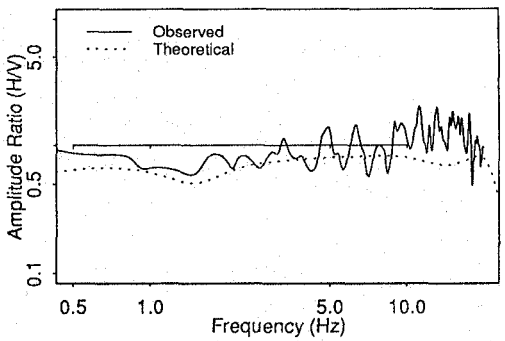

Fig. 6 Average amplitude ratio together with theoretical Rayleigh-wave at the reference point

accelerometers and circled numbers are microtremor pickups). Three case s of microtremor array were measured, namely, case A (vertical component), case B (horizontal component) and case C (both the vertical and the horizontal components along the arm 3). Also a reference point (9.8 m away from the model structure) was selected for checking the stability of the microtremor measurement at the site. At this point, microtremor observations were recorded for 2 minutes each hour for 24 hours (from 4:00 P.M. of 5th to 3:00 P.M. of 6th October, 1994) by using the built-in clock of the personal computer.

4.1 *Stability analysis*

For checking the stability of microtremor observation at the Hualien LSST site, 24 hour recording was made at the reference point as mentioned earlier. Obtained velocity records were converted from time domain to frequency domain to get the Fourier spectrum and were smoothed by using a Parzen window of bandwidth 0.4 Hz. Instead of using all the observed time records 6 time instants were selected for investigation. Figure 5 shows amplitude ratio (H/V) at the reference point for the 6 time instants. Although among these time instants 3 were measured during night time and 3 at day time, the amplitude ratios are almost stable.

Figure 6 shows amplitude ratio of microtremor together with theoretical Rayleigh-wave (fundamental mode) at the reference point. For H/V ratio of microtremor, $H = \sqrt{S_{NS} S_{EW}}$ and $V = S_{UD}$, where S_{NS}, S_{EW} and S_{UD} is average Fourier spectrum of NS, EW and UD components for 6 time instants, respectively. For the calculation of theoretical Rayleigh-wave amplitude ratio, the unified model (free-field) was used. It can be observed that the match between both observed and theoretical amplitude ratio is good over a wide frequency range.

4.2 *Comparison of microtremor with earthquake records*

The comparison of the properties of microtremor with those of the earthquake records was conducted in velocity. By integrating the recorded earthquake acceleration, the velocity of the earthquake ground motion was obtained. Figure 7 shows one example of the time histories of microtremor and earthquake for the three components.

The power spectra were calculated for both the microtremor and earthquake records by applying the smoothing process with a Parzen window of 0.4 Hz bandwidth. In the calculation of the power spectrum, for the earthquake ground motion full time window was employed and for microtremor 21 seconds was used. The power spectra for the three components of microtremor recorded at the reference point (pickups 6, 7 and 8 in Figure 2) are shown in Figure 8(a) and those calculated from the A13 accelerograph from EQ940120 are shown in Figure 8(b).

For all those 24 case s of microtremor observations at the reference point, power spectrum for NS-component was found to be lower than EW and UD-components. All of them have peaks around 1.2, 2.5 and 3.5 Hz. This may be the characteristics of this particular site.

However, in the case of earthquake records, the power spectrum of the vertical component has a smaller amplitude. For the three earthquake components no distinct peak can be observed. It is noticed that the power of the earthquake ground motion comes mainly from the S-wave in the horizontal components and from the P-wave in the vertical component. Hence, the power spectra of the vertical component and horizontal components reflect the different vibration properties of the site.

5 WAVE IDENTIFICATION AND DETERMINATION OF APPARENT WAVE VELOCITIES

There is some controversy about the microtremor wave type. For the determination of wave type both arrays of vertical and horizontal components were measured at the same points. The high-resolution frequency-wave number (FK) spectral analysis developed by Capon[10] were used to establish microtremor sources and to determine dispersion characteristics of this vertical

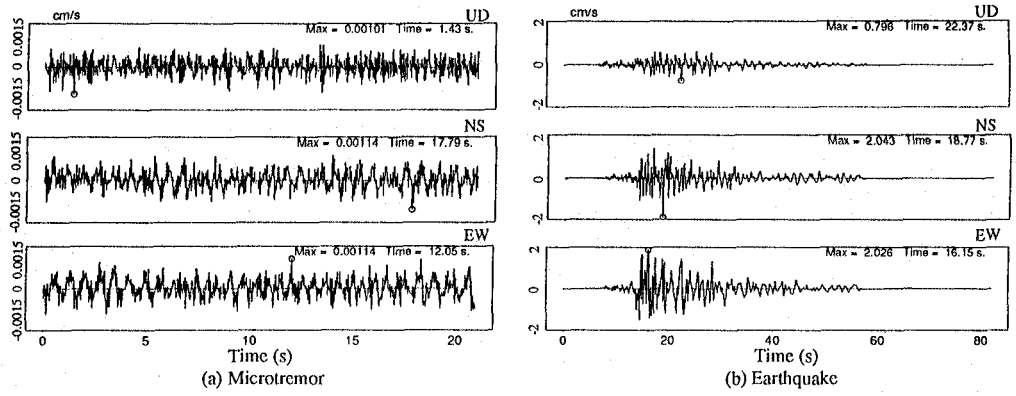

Fig. 7 Time histories of velocity for microtremor at the reference point and earthquake (EQ940120) at A13

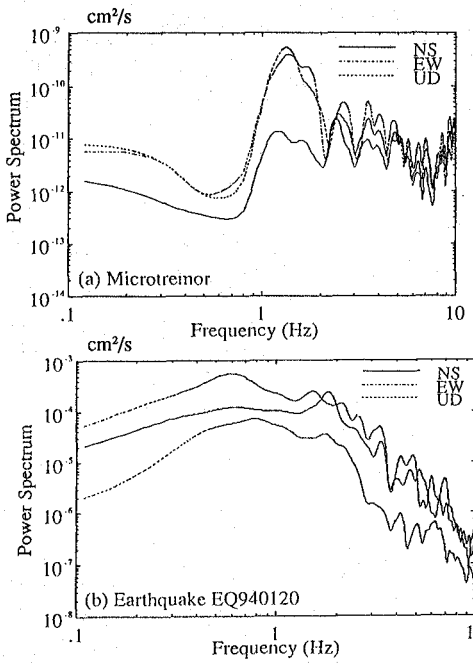

Fig. 8 Power spectra of three ground motion components at the reference point for microtremor and at A13 for earthquake

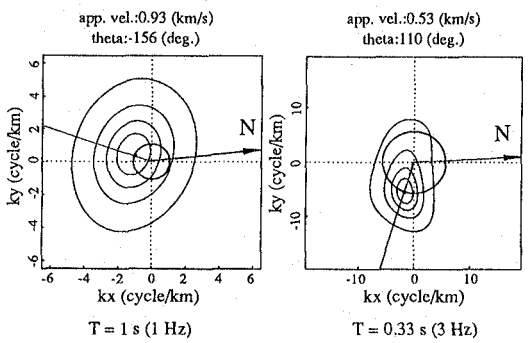

Fig. 9 FK-spectrum for some particular frequencies (vertical component)

and horizontal ground motions. Figure 9 shows FK spectral analysis for some particular frequencies of case A array. The frequencies corresponding to high coherency function and power spectrum amplitude were selected for FK-spectrum analysis.

5.1 *Measurement of vertical ground motion*

Figure 10(a) shows apparent velocities of microtremors for 3 time windows of a microtremor array (case A) together with theoretical dispersion curve of Rayleigh-wave (fundamental mode) based on the unified model. For these array observation, dispersion characteristics can only be obtained up to 10 Hz. Unfortunately for this site, it is not posssible to obtain dispersion characteristics above this frequency due to lack of space and position of the model and other structures at the site. The close resemblance between the theoretical curve and the microtremor observation, except for frequency 1.75 Hz can be attributed to the presence of Rayleigh-waves in the vertical components of microtremors. Figure 10(b) shows relation between azimuthal angles of observed microtremors with frequencies. The microtremor sources were stably distributed toward SE and SW directions in the frequency range of 2 to 7 Hz, because a marble plant is situated in those directions. For higher frequencies the sources vary randomly, as expected from high frequency microtremors. The spectral peak around frequency 1.75 Hz may be due to the construction of a model tank nearby or waves coming from some other unknown source along NE direction.

5.2 *Measurement of horizontal ground motion*

Some authors like Tamura et al.[11] showed that predominant period of ground can also be dominated by Love-wave. In array case B, NS component of

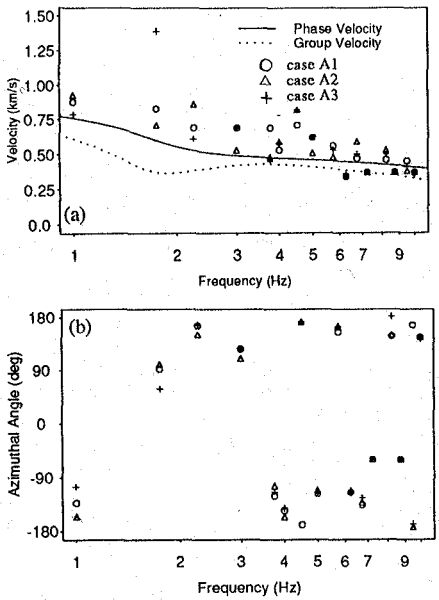

Fig. 10 (a) Apparent velocity together with theoretical dispersion curve for Rayleigh-wave (fundamental mode); (b) relation of azimuthal angles of observed microtremors with frequencies

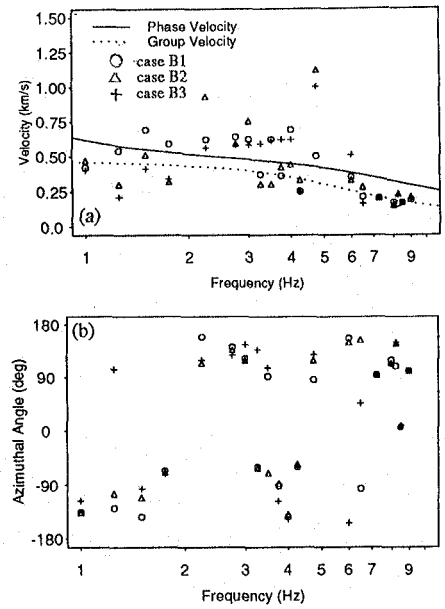

Fig. 11 (a) Apparent velocity together with theoretical dispersion curve for Love-wave (fundamental mode); (b) relation of azimuthal angles of observed microtremors with frequencies

microtremors was measured for this purpose.

Figure 11(a) shows theoretical dispersion characteristics of Love-wave together with observed dispersion curve and 11(b) shows relation between azimuthal angles and frequencies. Comparing observation and theoretical curve, it was found that for this site some low and high frequency microtremors may contain Love-wave but the middle range of frequency has little similarity with Love-wave. This middle range from 2.25 to 5 Hz waves was coming from the direction of marble plant. The other sources of microtremors are randomly distributed as can be observed from Figure 11(b).

6 AMPLIFICATION RATIO AT THE FREE-FIELD AND WITHIN THE BACKFILL

For investigating the effect of backfill as well as free-field soil-structure on microtremor observation 4 pairs of sensors (one UD and another NS) were placed along the arm 3 as shown in Figure 12.

The amplitude ratios (H/V) for three points are calculated and compared with the corresponding soil-structure models as described in Tables 2 to 4. These comparisons are shown in Figure 13. The theoretical amplitude ratio for fundamental mode Rayleigh-wave shows no clear peak due to the low impedance value between shear-wave velocity of top and base layer for the different underground models at this stiff soil site, which can be justified by the findings of previous studies[5,6]. The general characteristics of theoretical amplitude ratios for all the three models match with the observed one up to frequency of 4 Hz. For the free-field case (10.0 m away from the model structure) the match between them can be found for the whole frequency range. The reason for lack of match between theory and observation for higher frequency may be that microtremors consist of both Rayleigh and Love waves and is unseparable.

Figure 14 shows theoretical phase velocity versus frequency curve of fundamental mode Rayleigh-wave for the three soil-structure models as mentioned earlier. It can be seen that except beyond 10 Hz the three curves are almost the same. Beyond 10 Hz the differences are quite clear but due to lack of proper array data, we were unable to estimate apparent velocities in this range for observed microtremors.

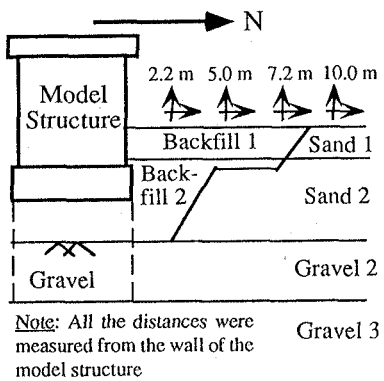

Fig. 12 Location of microtremor pickups for case C

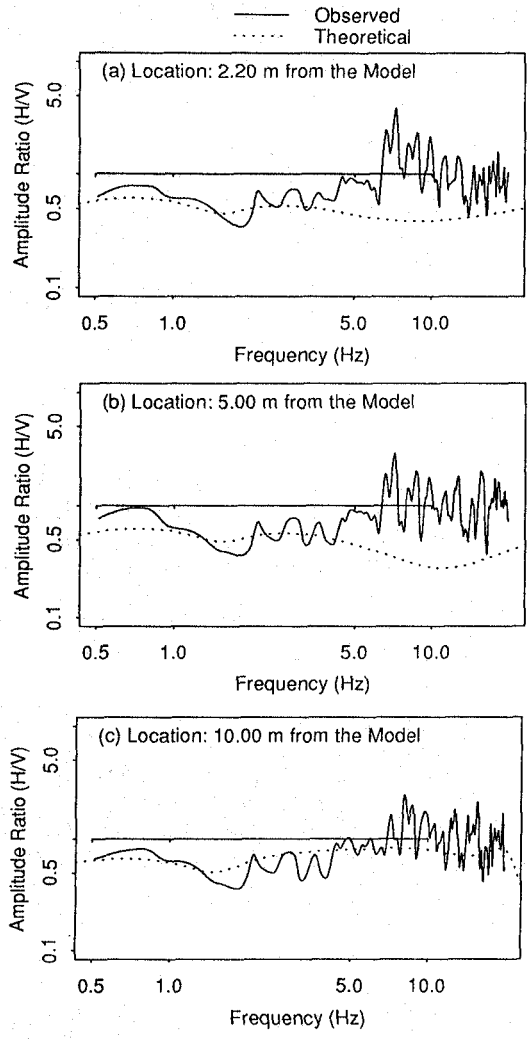

Fig. 13 Amplitude ratios (*H/V*) of microtremors plotted with theoretical Rayleigh-wave for different locations of case C

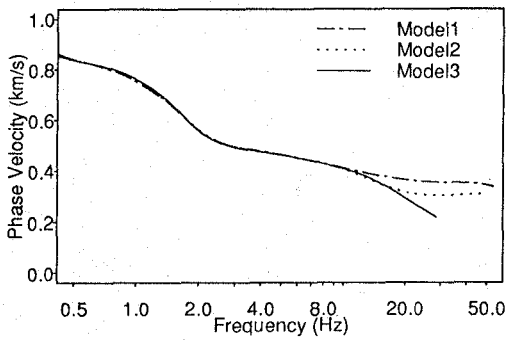

Fig. 14 Comparison among theoretical Rayleigh-wave dispersion curves based on three soil-structure models

7 CONCLUSIONS

Microtremors were observed as arrays and points at the locations of some surface accelerometers of Hualien LSST array. For this site, in the case of microtremors the power spectrum of the NS-component is lower than the EW and UD-components. At the reference point, the theoretical amplitude ratio of the fundamental Rayleigh-wave quite matches the observed average amplitude ratio of microtremor.

The microtremor observations of the ground gave reasonable phase velocities estimated from the free field soil properties. From the two types of array measurement, i.e., vertical and horizontal, it can be clearly observed that the microtremor is composed of Rayleigh-wave for a wide frequency range except for some low and high frequency microtremors, which may consist of Love-waves. Due to the low impedance ratio of the site and limitation of array layout, it was difficult to discuss the backfill soil properties clearly.

REFERENCES

1. H. T. Tang *et al.*, 'A large-scale soil-structure interaction experiment: Design and construction', *Nucl. eng. des.* **111**, 371-379 (1989).
2. T. Katayama, F. Yamazaki, S. Nagata, L. Lu and T. Turker,'A strong motion database for the Chiba seismometer array and its engineering analysis', *Earthquake eng. struct. dyn.*, **19**, 1089-1106 (1990).
3. H. T. Tang *et al.*, 'The Hualien large-scale seismic test for soil-stucture interaction research', *SMiRT 11 Transactions*, **K04/4**, 69-74 (1991).
4. Y. Nakamura,'A method for dynamic characteristics estimation of subsurface using microtremor on the ground surface', *QR of RTRI*, **30(1)**, 25-33 (1989).
5. T. Ohmachi, K. Konno, T. Endoh and T. Toshinawa,'Refinement and application of an estimation procedure for site natural periods using microtremor', *Journal of Civil Eng.*, **489(I-27)**, 251-260 (1994) (Japanese).
6. M. A. Ansary, M. Fuse, F. Yamazaki and T. Katayama,'Use of microtremors for the estimation of ground vibration characteristics', *Proc. 3rd Int. conf. on Recent Advances in Geotechnical Earthquake Eng. and Soil Dynamics* , **2**, 571-574 (1995).
7. F. Yamazaki, L. Lu, and T. Katayama,'Orientation error estimation of buried seismographs in array obserevation', *Earthquake eng. struct. dyn.*, **21**, 679-694 (1992).
8. T. Kokusho *et al.*,'Geotechnical investigation in the Hualien large-scale seismic test project', *SMiRT 12 Transactions*, **K03/4**, 85-90 (1993).
9. T. Kokusho *et al.*,'Soil-structure interaction research of a large-scale model structure at Hualien, Taiwan - (Part 1)', *Proc. 9th Japan earthquake eng. symp.* **II**, 1369-1374 (1994).
10. J. Capon,'High-resolution frequency-wavenumber spectrum analysis', *Proc. IEEE* **57(8)**, 1408-1418 (1969).
11. T. Tamura, O. Nagai, H. Kokubo, and H. Sumita,'Chracteristics of wave group of microtremors obtained by array measurement', *Journal of Structural and Construction Eng., AIJ*, **449**, 83-91 (1993) (Japanese).